Online March 26, 2022
Journal of Neuroendovascular Therapy 2022; 16: 395–401 DOI: 10.5797/jnet.oa.2022-0003

Original Article

Efficacy of Post-Dilatation during Carotid Artery Stenting for Unstable Plaque Using a Double-Layer Stent Evaluated by OFDI

Ryuichiro Kiyosawa, Takaya Saito, Shingo Yamada, and Kei Harada

Objective: This study aimed to use optical frequency domain imaging (OFDI) to evaluate the efficacy of post-dilatation (PD) after stent placement for unstable plaques during carotid artery stenting (CAS) using a double-layer stent.
Methods: Twelve unstable carotid plaque lesions diagnosed by MRI were evaluated using OFDI during CAS. The pre-procedural minimum lumen diameter was 1.6 ± 0.7 mm. Each lesion was pre-dilated with balloon catheters (diameter, 5.3 ± 0.5 mm), and a double-layer stent was deployed. PD was performed with balloon catheters of the same size as those used for pre-dilatation. Cross-sectional OFDI images within the stented segment were evaluated at 1-mm intervals for a 20-mm segment, including the most stenotic lesion. Slice rates for the presence of in-stent plaque protrusion (PP) and plaque between the double-layer lumen were calculated.
Results: No procedural complications occurred with the use of an embolic protection device. Compared to after stent placement, slice rates for any PP (44 ± 19% to 62 ± 22%, P <0.05) and plaque between the double-layer lumen (79 ± 16% to 91 ± 34%, P <0.05) were significantly increased after PD; slice rates for >500 μm PP (7.5 ± 14% to 0%, P <0.05) were significantly decreased. Visible debris were captured in 50% of lesions.
Conclusion: PD after double-layer carotid stent placement decreases in-stent large PP. Double-layer construction contributed to the prevention of large PP, as the PP may have been crushed into debris by PD.

Keywords carotid artery plaque, endovascular procedures, optical coherence tomography, self-expandable metal stent

Introduction

Carotid artery stenting (CAS) has become an effective alternative to carotid endarterectomy for stroke prevention in patients with carotid artery stenosis.[1] However, CAS for unstable plaques has been associated with a high risk of embolic complications.[2] In recent years, excellent embolic protection devices (EPDs) have overcome intraprocedural distal embolisms.[3] However, it has been observed that an in-stent plaque protrusion (PP) frequently occurs during CAS, especially in cases with unstable plaques, and causes intraprocedural and delayed embolic strokes.[4,5] Double-layer micromesh stents were developed to reduce the PP through the stent strut and distal embolism.[6,7] The Casper stent (Terumo, Tokyo, Japan), a double-layer micromesh stent, was developed to reduce PP through the stent strut as well as distal embolism.[8,9]

Post-dilatation (PD) during the CAS procedure helped in increasing in-stent lumen area; however, it increased procedure-related embolization because of fractured debris.[10,11] A previous report indicated that PD during CAS for unstable plaques using closed-cell design stents decreased large in-stent PP. Harada et al. reported in 2019 that PD during CAS for unstable plaques using closed-cell design stents significantly increased in-stent lumen area and apposition to the vessel wall; conversely, it decreased large in-stent PP and stent malapposition evaluated by optical coherence tomography (OCT).[11] However, the efficacy of PD for CAS using a double-layer stent has yet to be investigated. Therefore, the aims of this study were to use optical frequency domain imaging (OFDI) during CAS for unstable plaques using Casper stents to detect stent

Department of Neurosurgery, Fukuoka Wajiro Hospital, Fukuoka, Fukuoka, Japan

Received: January 15, 2022; Accepted: February 22, 2022
Corresponding author: Kei Harada. Department of Neurosurgery, Fukuoka Wajiro Hospital, 2-2-75, Wajirogaoka, Higashi-ku, Fukuoka, Fukuoka 811-0213, Japan
Email: keiharakeihara@yahoo.co.jp

dilatation, in-stent PP, plaque between double-layer lumen, and stent malapposition, and to evaluate the efficacy of PD.

Materials and Methods

From October 2020 to January 2021, 12 carotid lesions evaluated to be unstable by MRI were treated using Casper stents. Written informed consent was obtained from all patients. The research within our submission has been approved by the ethics institutional review board of our hospital (No. 00112). In symptomatic cases, CAS was performed at least 2 weeks after the onset of symptoms. The inclusion criteria were as follows: >80% asymptomatic internal carotid artery (ICA) stenosis and >50% symptomatic ICA stenosis. We did not include patients with creatinine levels >1.5 mg/dL and lesions with severe ICA elongation. In all lesions in which PD was performed with balloon catheters of the same size as those used during pre-dilatation, OFDI analysis was performed before pre-dilatation, after stent placement, and after PD. All patients were administered oral dual antiplatelet therapy with aspirin (100 mg/day) and clopidogrel (75 mg/day).

Plaque MRI

Carotid MRI using a 3-T imaging machine (Magnetom Verio; Siemens, Erlangen, Germany) was performed before CAS. T1- and T2-weighted images of the carotid artery, including the area with the highest rate of stenosis and plaque, were obtained. T1-weighted image parameters were repetition time (TR), 500; echo time (TE), 13; and slice thickness, 2.0 mm, and T2-weighted image parameters were TR, 4200; TE, 86; and slice thickness, 3.0 mm. The relative signal intensity (rSI) of plaque components was calculated in relation to the sternocleidomastoid muscle on T1-weighted images and in relation to the submandibular gland on T2-weighted images. On T1-weighted images, rSI >1.5 was defined as high, meaning unstable.

CAS procedure

Local anesthesia was administered to all patients to allow for monitoring of motor function and level of consciousness. Systemic anticoagulation was also achieved by the administration of heparin, maintaining an activated clotting time of at least 275 s. In all lesions, combined protection was performed using proximal protection and distal filter protection. In cases with easy arterial access to carotid lesion, 9-F Mo.Ma Ultra proximal protection device (Medtronic, Minneapolis, MN, USA) was used, and in cases with difficult arterial access to carotid lesion, an Optimo balloon guiding catheter (Tokai Medical Products, Aichi, Japan) was used because it was easy to navigate to the common carotid artery (CCA). In eight lesions, an 8–9 F guiding catheter with a temporary occlusion balloon was navigated to the CCA from the femoral artery. A PrecuSurge GuardWire (Medtronic) was inserted into the guiding catheter through a Y connector connected to the side of the guiding catheter and advanced to a point approximately 10 mm distal to the origin of the external carotid artery (ECA). The ECA was then occluded by inflating the PrecuSurge GuardWire to a 4–6 mm diameter. For the remaining four lesions, a 9-F Mo.Ma Ultra proximal protection device was navigated to occlude both the CCA and the ECA. A distal filter protection device (FilterWire EZ; Stryker, Fremont, CA, USA, or SpiderFX; Medtronic) was also crossed with the stenotic lesions. A 4 F to 6 F sheath was then deployed in the femoral vein.

The blood return system is a conduit that connects the side flow reverse port of the guiding catheter to the central venous system. Before reentering the venous system, the blood passes through the chamber with an external filter, which collects particulate debris that are too large to pass through its 200-μm pores.[12] The ECA was continuously occluded until PD was performed. Inflation of the occlusion balloons in the CCA was intermittently performed to maintain cerebral blood flow. Pre-dilatation was performed using a 4.0–6.0 mm balloon catheter with a nominal pressure of 8 atm. Afterward, a Casper stent was deployed. PD was performed using balloon catheters of the same size as those used during pre-dilatation with a nominal pressure of 8 atm for 20 s at one time. PD was performed with these steps at least thrice. During PD, bradycardia with a heart rate of less than 40 occurred in two cases, and those showed rapid recovery after deflation of the balloon without venous injection of atropine. Visible debris captured by the external filter and/or distal filters was checked.

Diffusion-weighted (DW) MRI was performed within 1–2 days after CAS. Carotid ultrasound or CTA was performed to examine restenosis and in-stent thrombosis during a follow-up period of at least 6 months. Dual oral antiplatelet therapy was continued for at least 3 months, and dual oral antiplatelet regimens were discontinued when in-stent PP or restenosis was not detected upon ultrasound or CTA examination. In these cases, a single oral antiplatelet regimen was continued instead.

OFDI technique

OFDI was performed using a Lunawave OFDI system (Terumo). An OFDI imaging catheter (FastView; Terumo) was advanced into the carotid artery using a 0.014-inch micro guidewire or filter protection device. Carotid OFDI imaging was performed pre-procedure, after stent placement, and after PD. Pullbacks were started while the CCA was occluded with manual injection of 20 mL of 50% saline diluted contrast medium (iodixanol 270 mg/mL) for approximately 5 s to completely replace blood from the artery. These injections were performed using a guide catheter. After stent deployment and after PD, the same OFDI maneuvers were repeated.

Quantitative software (Lunawave Offline Viewer; Terumo Corp.) was used for offline OFDI analysis by two experienced OFDI readers. Cross-sectional OFDI within the stented segment of the ICA was evaluated at 1-mm intervals for the presence of PP, plaque between the double-layer lumen, and stent malapposition. The corresponding arterial segment in the pre-stent images was identified using anatomical landmarks such as origin of ICA and analyzed at similar 1-mm intervals. PP was defined as the protrusion of tissues between the stent struts extending inside a circular arc. The distance from the arc to the greatest extent of protrusion was measured. Malapposition was defined as the distance measured from the surface of the blooming to the lumen contour, which was greater than the total thickness of the stent strut plus one-half of the blooming. A well-apposed strut had a protrusion distance ranging from 10 to 200 μm, and the malapposed strut had a protrusion distance of >200 μm.[13]

The OFDI evaluation, without artifacts, of continuous 20-mm-stented segments in both after stent placement and after PD, including pre-procedural most stenotic lesions, was carried out in this study.

Statistical analysis

Continuous variables, such as age and laboratory tests, were presented as mean (standard deviation [SD]). The chi-square analysis and Fisher's exact probability test were performed for categorical variables, such as the slice rates of PP or stent malapposition. $P < 0.05$ was considered significant.

Table 1 Patient characteristics, OFDI results, and clinical course

	n = 12
Characteristics	
Age, years	74 ± 6
Men	12
Clinical features	
Hypertension	8
Diabetes	4
Heart disease	4
Presenting event	
Minor ischemic stroke	4
Ocular ischemia	2
Asymptomatic	6
Laboratory tests	
Triglyceride, mg/dL	119 ± 77
LDL cholesterol, mg/dL	100 ± 42
MRI features	
T1W, rSI	1.9 ± 0.4
T2W, rSI	1.6 ± 0.5
Medication	
Aspirin	12
Clopidogrel	12
Statin	7
OCT results	
Plaque morphology	
Lipid	12
Calcification	2
Ulceration	8
TCFA	12
Disruption	10
Thrombus	2
Neovascularization	2
OFDI-NASCET, %	72 ± 13
Area of most stenotic lesions, mm^2	3.4 ± 1.8
Diameter of most stenotic lesions, mm^2	1.6 ± 0.7
Pre-dilatation and PD balloon size, mm	5.3 ± 0.5
Visible debris	6
Clinical course	
Neurological deficits	0
MRI–DWI high spots	5
Duration of DAPT, months	3.4 ± 1.0
Follow-up, months	9.7 ± 1.4
Restenosis	0
Delayed ischemic stroke	0

DAPT: dual antiplatelet therapy; LDL: low-density lipoprotein; MRI–DWI: magnetic resonance imaging–diffusion weighted imaging; NASCET: North American Symptomatic Carotid Endarterectomy Trial; OCT: optical coherence tomography; OFDI: optical frequency domain imaging; PD: post-dilatation; rSI: relative signal intensity; T1W: T1 weighted; T2W: T2 weighted; TCFA: thin-cap fibroatheroma

Results

Clinical results

Patient characteristics, the pre-procedural OFDI findings, and clinical results are given in **Table 1**. In symptomatic patients, the mean time lapsed from the qualifying event to the CAS procedure was 23 days (range, 14–60 days). Successful revascularization with <30% residual stenosis in each case was confirmed by angiography. No technical or neurological complications occurred during OFDI

Table 2 OFDI findings after post stent placement and after PD

	Post-stent placement	PD	P value
Minimum lumen			
Diameter, mm	3.0 ± 0.7	3.7 ± 0.8	<0.001
Area, mm^2	9.1 ± 2.9	13.7 ± 5.4	<0.001
Number of >500-μm PP, n	5	0	<0.05
Rate of slices (%)			
Any PP, %	44 ± 19	62 ± 22	<0.05
>500-μm PP, %	7.5 ± 14	0	<0.05
Plaque between the double layer space, %	79 ± 16	91 ± 15	<0.05
Malapposition, %	78 ± 25	53 ± 34	<0.05

OFDI: optical frequency domain imaging; PD: post-dilatation; PP: plaque protrusion

pullback and CAS procedures. The total amount of contrast medium during the CAS procedure was 60–90 mL. A high signal on DW-MRI was detected in five out of 12 (42%) patients, and all were asymptomatic. Post-procedural ischemic neurological deficits, access site complications, and cardiac events were not observed during the follow-up period. Restenosis was not detected in any lesions examined by ultrasound or upon CTA examination.

OFDI results

OFDI findings of a comparison between after stent placement and after PD are given in **Table 2**. Minimum lumen diameters, areas, and mean lumen areas were significantly larger after PD compared to those after stent placement. Compared to after stent placement, the slice rates of in-stent PP and plaque between the double-layer lumens were significantly increased after PD; >500 μm PP and stent malapposition were significantly decreased. A representative case showing that >500 μm PP decreased after PD is shown in **Fig. 1**. A representative case showing that plaque between the double-layer lumens increased after PD is shown in **Fig. 2**.

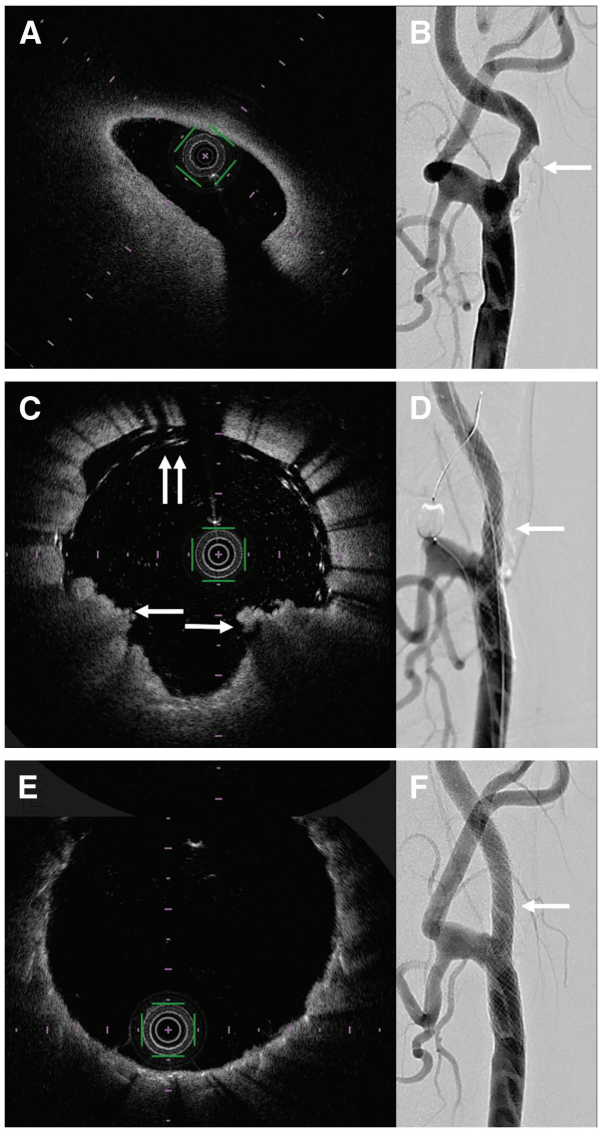

Fig. 1 Representative case showing that in-stent large PP (>500 μm) is decreased after PD. (**A**) Pre-procedural OFDI shows homogenous, diffuse border without surface signal-rich regions, which indicated lipid-rich plaque with thin-cap fibroatheroma. (**B**) Angiogram of pre-procedural carotid stenosis. (**C**) After pre-dilatation (5.0-mm balloon) and double-layer stent placement, large PP (arrows) between the struts was observed by OFDI. The double arrows indicate stent malapposition. The space between the double-layer structure was not clear. (**D**) Angiogram after stent placement. (**E**) After PD, in-stent large PP decreased, while in-stent small PP increased by OFDI analysis. (**F**) Post-procedural angiogram revealed good revascularization. Arrows in (**B**), (**D**), and (**F**) indicate the corresponding locations of OFDI analysis. OFDI: optical frequency domain imaging; PD: post-dilatation; PP: plaque protrusion

Discussion

In this study, it was observed that any PP and plaque between the double-layer lumens were significantly higher after PD compared to after stent placement for unstable plaque using a double-layer stent; however, >500 μm PP and stent malapposition were significantly less. This suggests that the double-layer structure contributed to protecting the PP and PD reduced in-stent large PP. A similar result that PD reduces >500 μm PP through stent struts for carotid unstable plaque using a closed-cell stent was observed in this study even while using a double-layer stent.[11]

OCT/OFDI is a progressively accepted intravascular modality for studying coronary arteries. It provides

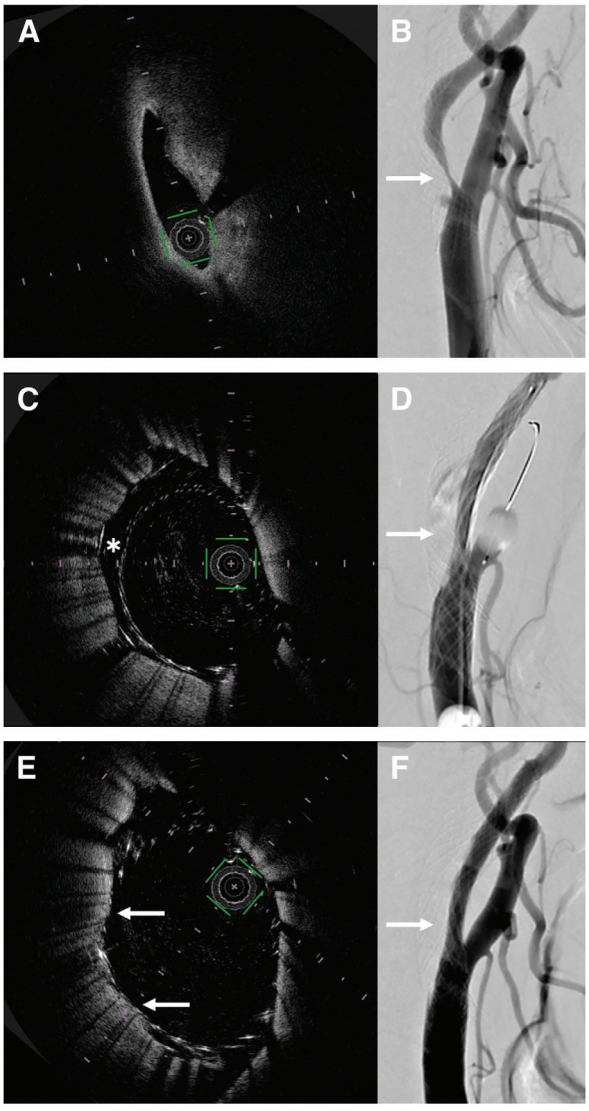

Fig. 2 Representative case showing plaque sealing between double-layer lumen after PD. (**A**) Pre-procedural OFDI indicated plaque disruption. (**B**) Angiogram of pre-procedural carotid stenosis. (**C**) After pre-dilatation (5.0-mm balloon) and after double-layer stent placement, no plaque was observed in the double-layer space (*). (**D**) Angiogram after stent placement. (**E**) After PD, plaque in the double-layer lumen increased. Plaque was well sealed between the double-layer lumen (arrows). After PD, the border of the double-layer stent strut was not clear. Arrows in (**B**), (**D**), and (**F**) indicate the corresponding locations of OFDI analysis. OFDI: optical frequency domain imaging; PD: post-dilatation

unprecedented microstructural information regarding atherosclerotic plaques and placed stents, and has a high-resolution capacity of 10 mm. OCT/OFDI has been used to assess atherosclerotic carotid plaque morphology, PP, and stent apposition. Several reports have been made on the safety of OCT-guided CAS.[3,4,13)]

In-stent PP could cause post-procedural embolism after CAS using a conventional open-cell stent.[4,14,15)] Additionally, even a closed-cell stent, which was expected to prevent PP for unstable carotid lesions, could not overcome this problem.[4)] In the previous study about OCT analysis during CAS using a closed-cell stent for 14 unstable plaques, any PP was observed in all lesions and PP >500 μm was observed in 50% of carotid lesions.[4)]

Double-layer micromesh stents have been developed to reduce PP during CAS, including the CGuard stent (InspireMD, Tel Aviv, Israel), RoadSaver/Casper stent, and Gore stent (W.L. Gore and Associates, Flagstaff, AZ, USA).[6,7,16,17)] They have a micromesh made of nitinol placed inside a closed-cell design stent frame. Their stent frame strut thickness is 180 μm, and their metal mesh strut size and pore size are 42 μm and 375 μm, respectively.[6,16)] However, previous OCT/OFDI studies suggested that PP was observed even when using double-layer stents.[16,18)] Yamada et al. reported using OFDI analysis that the presence of PP was apparently lower in the Casper stent group (44%) than that in the conventional (single-layer) stent group (88%). Umemoto et al. reported that PP was observed using both CGuard stents and RoadSaver stents, which are both double-layer stents, with OCT analysis.[16)] In this study, PP was observed in five out of 12 lesions after stent placement and in none of the lesions after PD. In percutaneous coronary artery stent placement, balloon dilatation time and pattern affect stent diameter; furthermore, multiple repetitive short balloon inflations result in a larger stent lumen gain compared to a single prolonged inflation amounting to the same cumulative time.[19)] In CAS using the Casper stent, whether PD contributed to in-stent PP being crushed or not was not reported; however, PD was thought to contribute to an increase in in-stent lumen and crushing of in-stent PP.

From these OFDI findings, we speculate the following: First, after stent placement, the space in the double-layer lumen was wide, especially in the stenotic lesions, because the inner stent strut was not sufficiently expanded despite the use of a large-diameter balloon (mean diameter, 5.3 mm). After stent placement, many plaques remain outside the stent; however, soft plaque can protrude into the in-stent lumen as PP or debris. Second, PD contributes to the expansion of stent struts and compresses the double-layer lumen; conversely, parts of the plaque protrude into the in-stent lumen through the stent strut. Third, large PP was crushed as debris, and small PP (<100 μm) remained around the stent strut. In this study, delayed in-stent PP was not observed in imaging during at least a 6-month follow-up

period. The double-layer structure is thought to chronically contribute to plaque stabilization.

We considered that PD should be performed to increase in-stent lumen diameter and decrease large in-stent PP even in cases of unstable plaque lesions in which sufficient EPD, such as proximal protection, which can retrieve more debris than distal filter protection, is achieved.[10] In cases where large PP was observed after Casper stent placement, which causes delayed migration, additional PD should be primarily performed to reduce PP. In contrast, PD might not be avoided in cases of unstable plaque in which sufficient EPD is not achieved, including cases that only make use of distal filter protection.

This study had some limitations. This was a single-center study conducted with a limited number of patients. There was no control group in this study, and the selected lesions predominantly comprised unstable plaques, non-elongated lesions, and lesions treated with same-sized balloon catheters pre-dilatation and PD. MRI is a well-established imaging modality for carotid plaque characterization. Plaque imaging using R1-weighted MRI has a very high sensitivity for detecting unstable plaques that reflect lipid-rich plaques and hemorrhages.[20] In this study, rSI >1.5 of T1WI obtained with 3.0-T MRI was defined as unstable plaque to increase the sensitivity of the assumed unstable plaque. Limitations regarding the construction of the Casper stent are as follows. In the previous study on PP after closed-cell stent placement evaluated by OCT analysis, the area of the stent cells with PP was calculated;[4] however, in this study, the area of the stent cells with PP could not be calculated because the double-layer stent strut was too small. In the previous study on PP after PD using a closed-cell stent, the area of in-stent PP on OCT slices was calculated; however, in this study, this was difficult because the precise border of the in-stent lumen and thin stent strut of the double-layer construction was difficult.

Conclusion

After PD for carotid unstable plaque using the Casper stent, we observed that the in-stent lumen area, small PP, and plaque between the double-layer lumen increased; however, >500 μm PP and stent malapposition decreased. PD may decrease delayed ischemic events by expanding the stent and decreasing in-stent large PP, subsequently crushing in-stent PP into the in-stent lumen as debris. In-stent PP was less than that using a closed-cell stent; the double-layer construction of the stent contributes to protection from in-stent PP. However, in CAS for unstable plaque with PD, sufficient EPD was needed to prevent intraprocedural embolization even with the use of a double-layer stent.

Acknowledgments

The authors thank Toshiya Morinaga (medical engineer of Fukuoka Wajiro Hospital) for help with the analysis of OCT frames.

Disclosure Statement

This research did not receive any specific grant from funding agencies in the public, commercial, or not-for-profit sectors.

References

1) Rosenfield K, Matsumura JS, Chaturvedi S, et al. Randomized trial of stent versus surgery for asymptomatic carotid stenosis. *N Engl J Med* 2016; 374: 1011–1020.
2) Yamada K, Yoshimura S, Kawasaki M, et al. Embolic complications after carotid artery stenting or carotid endarterectomy are associated with tissue characteristics of carotid plaques evaluated by magnetic resonance imaging. *Atherosclerosis* 2011; 215: 399–404.
3) Knappich C, Kuehnl A, Tsantilas P, et al. The use of embolic protection devices is associated with a lower stroke and death rate after carotid stenting. *JACC Cardiovasc nterv* 2017; 10: 1257–1265.
4) Harada K, Oshikata S, Kajihara M. Optical coherence tomography evaluation of tissue prolapse after carotid artery stenting using closed cell design stents for unstable plaque. *J Neurointerv Surg* 2018; 10: 229–234.
5) Funatsu N, Enomoto Y, Egashira Y, et al. Tissue protrusion with attenuation is associated with ischemic brain lesions after carotid artery stenting. *Stroke* 2020; 51: 327–330.
6) Wissgott C, Schmidt W, Brandt C, et al. Preliminary clinical results and mechanical behavior of a new double-layer carotid stent. *J Endovasc Ther* 2015; 22: 634–639.
7) Nerla R, Castriota F, Micari A, et al. Carotid artery stenting with a new-generation double-mesh stent in three high-volume Italian centres: clinical results of a multidisciplinary approach. *EuroIntervention* 2016; 12: e677–e683.
8) Bosiers M, Deloose K, Torsello G, et al. The CLEAR-ROAD study: evaluation of a new dual layer micromesh stent system for the carotid artery. *EuroIntervention* 2016; 12: e671–e676.

9) Imamura H, Sakai N, Matsumoto Y, et al. Clinical trial of carotid artery stenting using dual-layer CASPER stent for carotid endarterectomy in patients at high and normal risk in the Japanese population. *J Neurointerv Surg* 2021; 13: 524–529.
10) Montorsi P, Caputi L, Galli S, et al. Microembolization during carotid artery stenting in patients with high-risk, lipid-rich plaque. A randomized trial of proximal versus distal cerebral protection. *J Am Coll Cardiol* 2011; 58: 1656–1663.
11) Harada K, Kajihara M, Sankoda Y, et al. Efficacy of post-dilatation during carotid artery stenting for unstable plaque using closed-cell design stent evaluated by optical coherence tomography. *J Neuroradiol* 2019; 46: 384–389.
12) Harada K, Kakumoto K, Morioka J, et al. Combination of flow reversal and distal filter for cerebral protection during carotid artery stenting. *Ann Vasc Surg* 2014; 28: 651–658.
13) de Donato G, Pasqui E, Alba G, et al. Clinical considerations and recommendations for OCT-guided carotid artery stenting. *Expert Rev Cardiovasc Ther* 2020; 18: 219–229.
14) Beppu M, Mineharu Y, Imamura H, et al. Postoperative in-stent protrusion is an important predictor of perioperative ischemic complications after carotid artery stenting. *J Neuroradiol* 2018; 45: 357–361.
15) Kotsugi M, Takayama K, Myouchin K, et al. Carotid artery stenting: investigation of plaque protrusion incidence and prognosis. *JACC Cardiovasc Interv* 2017; 10: 824–831.
16) Umemoto T, de Donato G, Pacchioni A, et al. Optical coherence tomography assessment of newgeneration mesh-covered stents after carotid stenting. *EuroIntervention* 2017; 13: 1347–1354.
17) Stabile E, de Donato G, Musialek P, et al. Use of dual-layered stents in endovascular treatment of extracranial stenosis of the internal carotid artery: results of a patient-based meta-analysis of 4 clinical studies. *JACC Cardiovasc Interv* 2018; 11: 2405–2411.
18) Yamada K, Yoshimura S, Miura M, et al. Potential of new-generation double-layer micromesh stent for carotid artery stenting in patients with unstable plaque: a preliminary result using OFDI Analysis. *World Neurosurg* 2017; 105: 321–326.
19) Skowronski J, Wolny R, Jastrzebski J, et al. Impact of balloon inflation time and pattern on coronary stent expansion. *J Interv Cardiol* 2019, 6945372.
20) Yoshida K, Narumi O, Chin M, et al. Characterization of carotid atherosclerosis and detection of soft plaque with use of black-blood MR imaging. *AJNR Am J Neuroradiol* 2008; 29: 868–874.